BBA - Molecular Basis of Disease 1865 (2019) 165540

Contents lists available at ScienceDirect

BBA - Molecular Basis of Disease

journal homepage: www.elsevier.com/locate/bbadis

# G-MDSC-derived exosomes attenuate collagen-induced arthritis by impairing Th1 and Th17 cell responses

Dongwei Zhu[a,b], Jie Tian[b], Xinyu Wu[b], Min Li[b], Xinyi Tang[a], Ke Rui[c], Hongye Guo[b], Jie Ma[b], Huaxi Xu[b], Shengjun Wang[a,b,*]

[a] Department of Laboratory Medicine, The Affiliated People's Hospital, Jiangsu University, Zhenjiang, China
[b] Department of Immunology, Jiangsu Key Laboratory of Laboratory Medicine, School of Medicine, Jiangsu University, Zhenjiang, China
[c] Department of Laboratory Medicine, The Affiliated Hospital of Jiangsu University, Zhenjiang, China

ARTICLE INFO

*Keywords:*
Myeloid-derived suppressor cells
Exosomes
MicroRNA
Collagen-induced arthritis

ABSTRACT

The therapeutic effect of myeloid-derived suppressor cells (MDSCs) in mice with collagen-induced arthritis (CIA) remains controversial. We analyzed the role of exosomes derived from granulocytic MDSCs (G-MDSCs) in CIA and explored the potential mechanism underlying the immunosuppressive effect. In CIA mice, G-MDSC-derived exosomes (G-exo) efficiently reduced the mean arthritis index, leukocyte infiltration and joint destruction. G-exo decreased the percentages of Th1 and Th17 cells both in vivo and in vitro. The miR-29a-3p and miR-93-5p contained in G-exo were verified to inhibit Th1 and Th17 cell differentiation by targeting T-bet and STAT3, respectively. Notably, the delivery of exogenous miR-29a-3p and miR-93-5p enhanced the ability of bone marrow-derived G-exo to attenuate arthritis progression in CIA mice. Exosomes derived from human MDSCs, which overexpressed miR-29a-3p and miR-93-5p, suppressed Th1 and Th17 cell differentiation in vitro. These data showed that G-exo alleviated CIA by suppressing Th1 and Th17 cell responses. Mechanistically, miR-29a-3p and miR-93-5p were verified to inhibit the differentiation of Th1 and Th17 cells, respectively. Our findings demonstrated the therapeutic potential of G-MDSC-derived exosomal miRNAs in autoimmune arthritis.

## 1. Introduction

Rheumatoid arthritis (RA) is a systemic autoimmune disease characterized by the destruction of bone and cartilage, which results in deformity and disability of the joints [1]. The disruption of the immune balance by proinflammatory Th1 and Th17 cells contributes to the progression of RA patients or animal model [2–4]. Traditional drugs have severe side effects, and the currently available immunotherapy is simple but expensive [5,6].

Myeloid-derived suppressor cells (MDSCs) are a heterogeneous cell population derived from myeloid cells that proliferate extensively under the pathological conditions associated with tumors, infections, autoimmune diseases and trauma [7,8]. MDSCs can be divided into two subtypes according to cell morphology and the surface expression of Gr-1 (consisting of Ly-6G and Ly-6C); granulocyte-like cells with the $CD11b^{+}Ly6G^{+}Ly6C^{low}$ phenotype are identified as granulocytic MDSCs (G-MDSCs), and monocyte-like cells with the $CD11b^{+}Ly6G^{-}Ly6C^{high}$ phenotype are identified as monocytic MDSCs (M-MDSCs) [9]. Because of their powerful immunosuppressive ability, MDSCs were administered to mice with collagen-induced arthritis (CIA). The results suggested that MDSCs inhibit $CD4^{+}$ T cell inflammation and reduce the severity of CIA and that the severity of the disease could be alleviated by the adoptive transfer of MDSCs [10]. Although MDSCs are used to treat autoimmune diseases, the biological roles of MDSCs in CIA are unclear, and the clinical application of MDSCs remains controversial [11–14].

Exosomes are bioactive vesicles with a diameter of 30–150 nm that are secreted by many types of cells and present in various body fluids [15,16]. A variety of lipids, proteins and nucleic acids are contained in exosomes [16]. Exosomes can transfer their cargo to recipient cells, thus contributing to intercellular signaling [16]. Attempts have been made to use exosomes as therapeutic agents because they have low cytotoxicity, pose a low biohazard risk and have the potential to target specific tissues and organs. Our previous study showed that G-MDSC-derived exosomes (G-exo) could attenuate DSS-induced colitis by promoting T regulatory cell (Treg) expansion and inhibiting Th1 cell proliferation [17]. MicroRNAs (miRNAs) are small noncoding RNAs that can be loaded into exosomes. A recent study demonstrated critical effects of exosomal miRNAs on recipient cells, such as promoting cell migration, enhancing tube formation and stimulating the immune

* Corresponding author at: Department of Laboratory Medicine, The Affiliated People's Hospital, Jiangsu University, Zhenjiang 212013, China.
*E-mail address:* sjwjs@ujs.edu.cn (S. Wang).

https://doi.org/10.1016/j.bbadis.2019.165540
Received 15 May 2019; Received in revised form 22 August 2019; Accepted 25 August 2019
Available online 27 August 2019
0925-4439/ 

response [18]. Treg-derived exosomes containing Let-7d have been reported to suppress Th1 cell proliferation and alleviate inflammatory bowel disease [19]. Furthermore, exosomal miR-24-3p was reported to impede T cell differentiation and proliferation by targeting FGF11 in nasopharyngeal carcinoma [20].

In this study, we investigated the effect of G-exo on CIA. The results showed that miR-29a-3p and miR-93-5p contained in G-exo suppressed Th1 and Th17 cell responses and attenuated arthritis progression in CIA mice. Our findings imply that miRNA-containing G-exo can potentially be used as an immunotherapeutic agent in autoimmune arthritis.

## 2. Materials and methods

### 2.1. Induction of CIA

CIA was induced in 8-week-old male DBA/1 mice by immunization with bovine type II collagen (C-II) using our previously described protocol [4]. Briefly, the CIA mouse model was generated by immunizing DBA/1 mice with an initial immunization consisting of 100 μl of C-II (Chondrex, USA) emulsion (1 mg/ml) in complete Freund's adjuvant (CFA, 2 mg/ml; Difco, Detroit, MI) and a second immunization with 100 μl of C-II emulsion (1 mg/ml) in Freund's incomplete adjuvant (FIA). CIA mice were injected intravenously with exosomes (100 μg/mouse/injection) on days 18 and 24. The mice were monitored every three days, and the scores were assigned as follows: 0 = normal, 1 = erythema, 2 = erythema plus swelling, 3 = extension/loss of function, and the total score = sum of the scores of 4 limbs. All animal experiments performed in this study were approved by the Jiangsu University Animal Ethics and Experimentation Committee.

### 2.2. Histopathological assessment

Sections (4 μm) of the joints were stained with hematoxylin and eosin (H&E) and scored for changes in synovial hyperplasia, cell infiltration, pannus formation, inflammation and bone erosion, each was scored as previously described [21,22]. Synovial hyperplasia was scored 0–3 as follows: 0 = normal, 1 = slight synovial cell proliferation (2–4 layers of synovial cells), 2 = mild synovial cell proliferation (> 4 layers of synovial cells), 3 = excessive synovial cell proliferation (erode cartilage and bone, and the joint space disappears). Cell infiltration was scored 0–3 according to the following criteria: 0 = normal, 1 = mild local infiltration, 2 = moderate local infiltration, 3 = extensive infiltration to articular capsule with the formation of condensates. Pannus formation was defined as synovial proliferation adjacent to cartilage and filling the joint space and was scored 0–3 as follows: 0 = none, 1 = minimal, 2 = moderate (invasion of < 50% of the cartilage surface), 3 = severe (invasion of > 50% of the cartilage surface). Inflammation was scored 0–4 as follows: 0 = normal, 1 = minimal inflammatory infiltration, 2 = mild infiltration, 3 = moderate infiltration with lymphoid aggregates, 4 = marked infiltration with lymphoid aggregates and edema. Bone erosion was scored 0–4 according to the following criteria: 0 = none, 1 = minimal (1–2 sites of resorption, visible only at high magnification), 2 = mild (at least 3 sites of resorption, visible only at high magnification), 3 = moderate (obvious foci of resorption, visible at low power), 4 = marked (large erosions extending through to the marrow space).

### 2.3. Exosome isolation

MDSCs, G-MDSCs, or M-MDSCs were isolated with an MDSC isolation kit (Miltenyi Biotec, Cologne, DE). MDSCs or MDSC subsets were cultured in medium without bovine serum exosomes for 24 h. An ExoQuick-TC™ Exosome Isolation Kit (SBI, CA, USA) was used to extract the exosomes from the culture supernatant.

### 2.4. Flow cytometric analysis

Surface markers were stained with fluorochrome-conjugated mAbs against the following proteins: CD11b, Ly-6G, Gr-1, CD4, CD33 (BioLegend, San Diego, CA), and HLA-DR (Invitrogen, USA). Intracellular staining, including staining for IFN-γ and IL-17A, was performed as previously described [23]. The differentiated cells were stimulated with PMA, ionomycin and monensin for 5 h before staining with intracellular antibodies. The stained cells were analyzed by flow cytometry (FCM) with a FACS Calibur (BD, USA), FlowSight (Merck Millipore, USA), or FACSCanto (BD, USA) flow cytometer.

### 2.5. T cell isolation and culture

Murine or human naïve $CD4^+$ T cells were isolated using a naïve $CD4^+$ T cell isolation kit (Miltenyi Biotec). In the differentiation assay, murine naïve $CD4^+$ T cells were polarized toward a Th1 phenotype by culture for 5 days with anti-CD28 (2 μg/ml) and anti-IL-4 (10 μg/ml) monoclonal antibodies (mAbs), IL-2 (10 ng/ml), and IL-12 (10 ng/ml) in a 24-well plate precoated with an anti-CD3 mAb (2 μg/ml). For murine Th17 cell differentiation, naïve $CD4^+$ T cells were cultured for 3 days with an anti-CD28 mAb (2 μg/ml), TGF-β (5 ng/ml), IL-6 (30 ng/ml), an anti-IL-4 mAb (5 μg/ml), an anti-IFN-γ mAb (5 μg/ml), and IL-23 (30 ng/ml) in a 24-well plate precoated with an anti-CD3 mAb (2 μg/ml).

To determine the suppressive effect of human MDSC-derived exosomes (Hu-MDSC-exo), human naïve $CD4^+$ T cells were polarized toward a Th1 phenotype by culture for 4 days with an anti-CD28 mAb (1 μg/ml) and IL-12 (5 ng/ml) in a 48-well plate precoated with an anti-CD3 mAb (1 μg/ml). For human Th17 cell differentiation, naïve $CD4^+$ T cells were cultured for 6 days with an anti-CD28 mAb (1 μg/ml), TGF-β (10 ng/ml), IL-6 (10 ng/ml), and IL-23 (20 ng/ml) in a 48-well plate precoated with an anti-CD3 mAb (1 μg/ml).

### 2.6. Reverse transcription-quantitative PCR

Reverse transcription-quantitative PCR (RT-qPCR) was used to detect the expression of miRNAs. Total RNA was extracted by TRIzol (Invitrogen, USA) and reverse transcribed with FSQ101 (Toyobo, Japan). PCR was performed with a 2720 Thermal Cycler (Thermo Fisher, USA). Real-time PCR was performed with Bio-Rad SYBR green mix (Bio-Rad, USA) according to the manufacturer's instructions.

### 2.7. Transfection and miRNA sequence analysis

The miR-22-3p, miR-16-5p, miR-29a-3p, and miR-93-5p mimics, as well as the miR-29a-3p and miR-93-5p inhibitors, were synthesized by RiboBio Co (Guangzhou, China). The transfection concentration of the mimics was 50 nM, while the inhibitors were used at a concentration of 100 nM. Naïve T cells and G-MDSCs were transfected with Entranster™-R (Engreen Biosystem Co., China) for 6 h. MiRNA sequence analysis was performed at RiboBio Co.

### 2.8. Western blot analysis

Exosomes or naïve $CD4^+$ T cells were lysed in radioimmunoprecipitation (RIPA) buffer. The lysates were separated by SDS-PAGE and transferred to PVDF membranes (Bio-Rad, Hercules, USA). The primary antibodies used included anti-CD9 (CST, USA), anti-CD63 (CST, USA), anti-calnexin (CST, USA), anti-phospho-STAT3 (CS, USA), anti-t-STAT3 (Santa Cruz, USA), and anti-T-bet (eBioscience, USA). Anti-rabbit HRP-conjugated and anti-mouse HRP-conjugated (CST, USA) secondary antibodies were used. Chemiluminescent detection (Champion Chemical, CA, USA) was used to visualize the bands on the PVDF membranes.

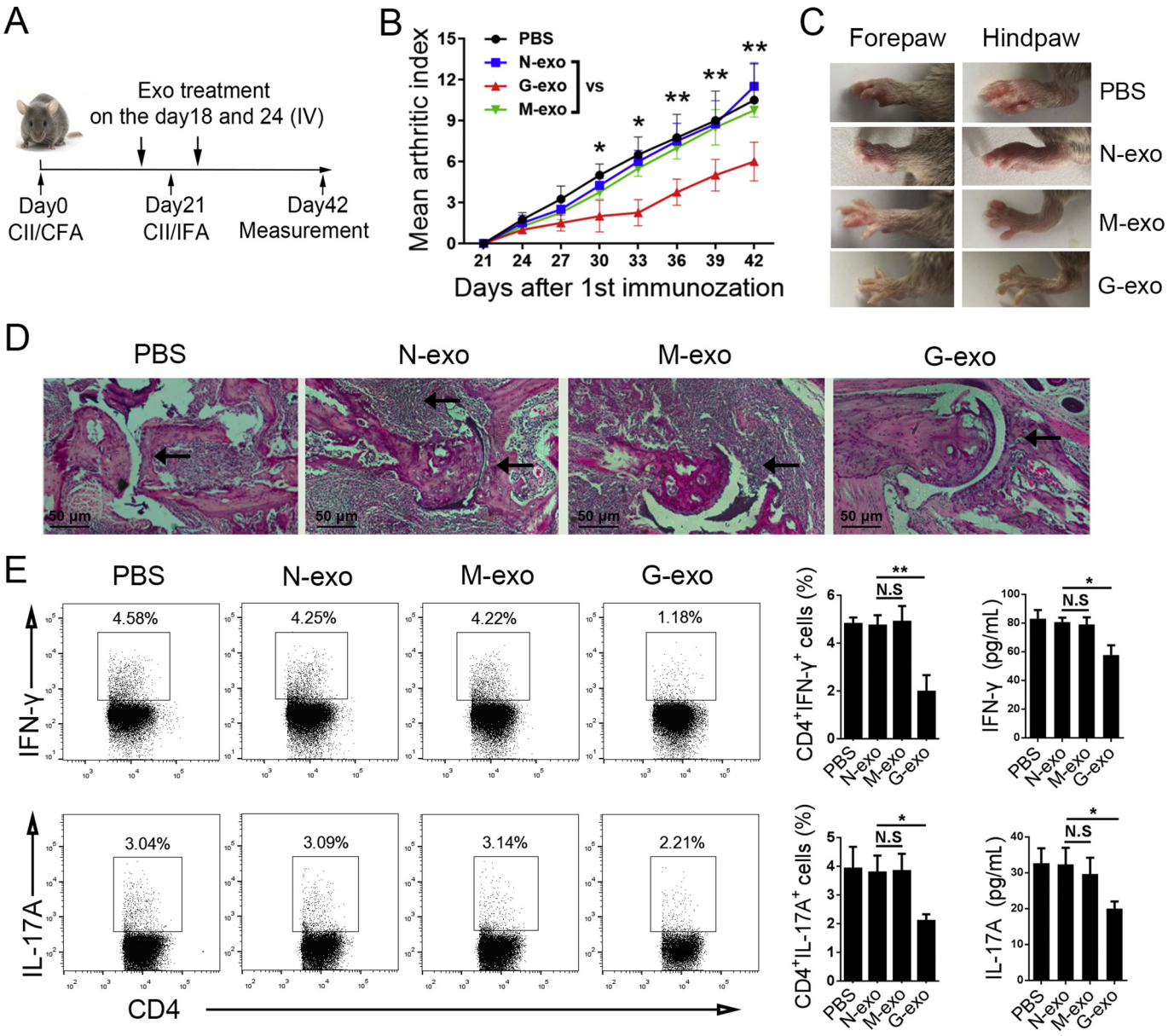


**Fig. 1.** G-MDSC-derived exosomes alleviate collagen-induced arthritis. (A) Schematic of CIA induction and exosome administration. CIA mice were intravenously injected with different exosomes (100 μg/mouse/injection) on days 18 and 24. The mice were sacrificed on day 42 for subsequent experiments ($n = 6$). (B) The MAI of CIA mice treated with PBS, N-exo, M-exo or G-exo was monitored every 3 days. (C) Representative images of the forepaws and hindpaws from the different groups are shown. (D) The joints were sectioned for hematoxylin-eosin staining. Representative sections of joint tissues are shown (original magnification, ×100). (E) The percentages of Th1 and Th17 cells in draining lymph nodes were analyzed by FCM (n = 6). The levels of serum IFN-γ and IL-17A were measured by an ELISA (n = 6). The values are the means ± SEM. ANOVA followed by Tukey's post-hoc analysis was used to compare three or more groups (B, E), $^{*}p < 0.05$, $^{**}p < 0.01$.

**Table 1**
Histological scores of ankle joints in MDSC-exosome-treated CIA mice.

| | Synovial hyperplasia | Cell infiltration | Pannus | Inflammation | Bone erosion |
|---|---|---|---|---|---|
| PBS | 2.50 ± 0.22 | 1.83 ± 0.30 | 2.34 ± 0.82 | 1.67 ± 0.37 | 2.50 ± 0.36 |
| N-exo | 2.67 ± 0.21 | 1.83 ± 0.17 | 2.50 ± 0.41 | 1.83 ± 0.26 | 2.33 ± 0.26 |
| M-exo | 2.33 ± 0.21 | 2.00 ± 0.26 | 2.16 ± 0.32 | 1.50 ± 0.67 | 2.16 ± 0.37 |
| G-exo | 1.17 ± 0.31$^{**}$ | 1.17 ± 0.17$^{*}$ | 1.00 ± 0.33$^{*}$ | 0.83 ± 0.12$^{**}$ | 1.17 ± 0.21$^{**}$ |

The value is the mean ± SEM (n = 6). ANOVA followed by Tukey's post-hoc analysis was used to compare three or more groups, $^{*}p < 0.05$, $^{**}P < 0.01$ (G-exo versus N-exo). Note: MDSC, myeloid-derived suppressor cells; CIA, collagen-induced arthritis; N-exo, exosomes derived from neutrophils; M-exo, exosomes derived from monocytic myeloid-derived suppressor cells; G-exo, exosomes derived from granulocytic myeloid-derived suppressor cells.

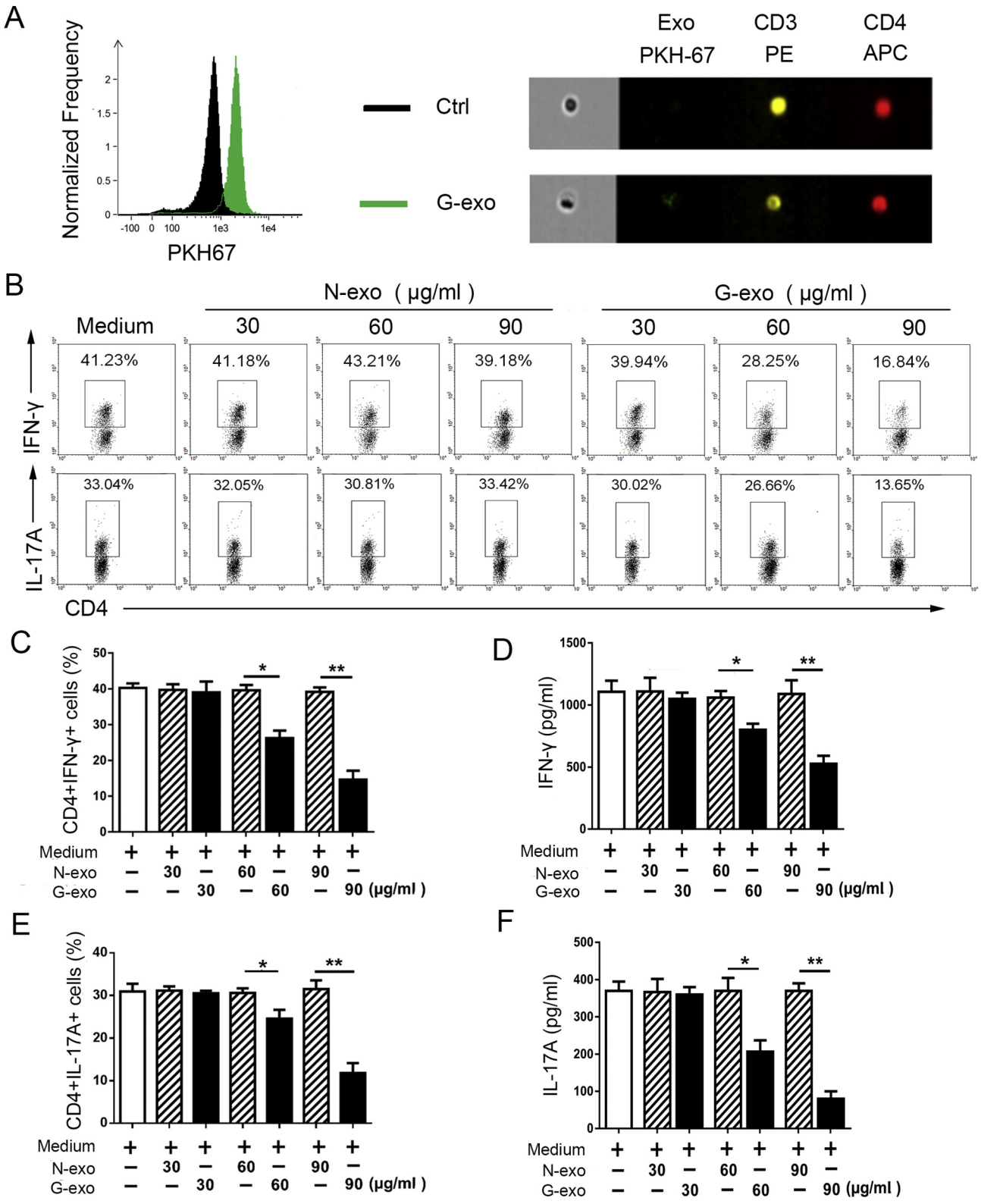


**Fig. 2.** G-MDSC-derived exosomes suppress Th1 and Th17 cell differentiation in vitro. (A) PKH67-labeled G-exo were added to murine naïve $CD4^+$ T cells for 24 h. Fluorescence-positive T cells were analyzed by FCM imaging with FlowSight (left); representative images are shown (right). (B) The proportions of Th1 and Th17 cells in the groups treated with G-exo or N-exo were analyzed by FCM ($n = 4$). (C, E) The results of the statistical analysis of Th1 and Th17 cell percentages are shown (n = 4). (D, F) The concentrations of IFN-γ and IL-17A in the culture supernatant were measured by ELISA ($n = 4$). The values are the means ± SEM. Statistics in C, D, E and F were performed using ANOVA followed by Tukey's post-hoc analysis. $^*p < 0.05$, $^{**}p < 0.01$.

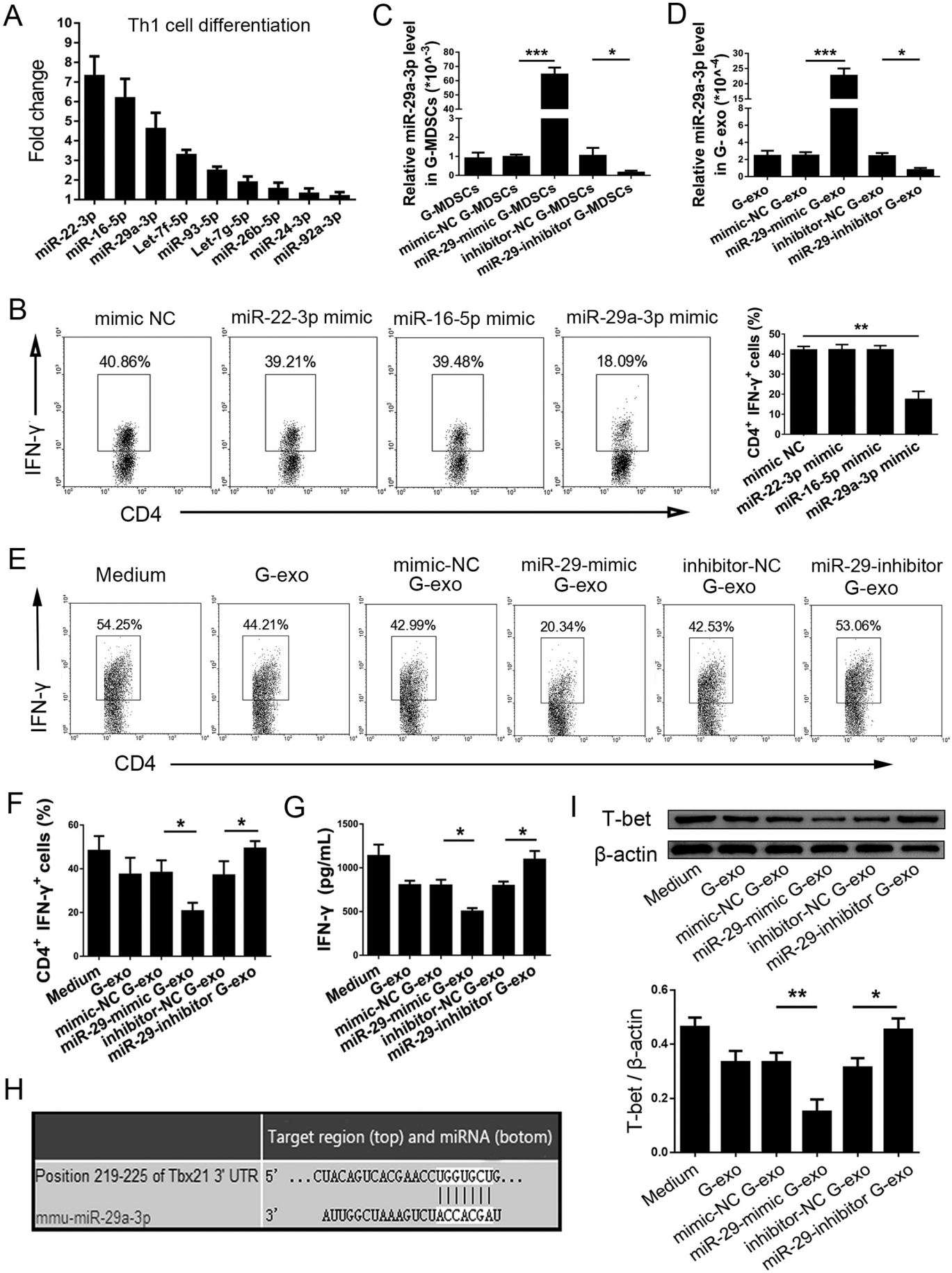


*(caption on next page)*

**Fig. 3.** MiR-29a-3p derived from G-MDSC-derived exosomes suppresses Th1 cell differentiation by targeting T-bet. (A) The fold changes of the 9 candidate miRNAs after G-exo treatment were determined by qRT-PCR. (B) Naïve $CD4^+$ T cells were induced to Th1 cells after transfection with mimic NC, miR-22-3p mimic, miR-16-5p mimic or miR-29a-3p mimic (n = 4). The percentages of Th1 cells were analyzed by FCM (left). The statistical analysis results are shown (right). (C, D) Mimic NC, miR-29a-3p mimic, inhibitor NC or miR-29a-3p inhibitor was transfected into G-MDSCs, and the miR-29a-3p levels in G-MDSCs (C) or G-exo (D) were measured by RT-qPCR (n = 4). (E) The frequencies of Th1 cells in the different groups treated with G-exo (n = 4) were analyzed by FCM. The statistical analysis of Th1 cell percentages (F) and IFN-γ concentrations (G) in the different groups is shown. (H) The miR-29a-3p target sequence in the 3′-UTR of T-bet was predicted with TargetScan. (I) The expression of T-bet in the different groups treated with G-exo was analyzed by western blotting (top), and the statistical analysis results are shown (bottom) ($n = 3$). The values are the means ± SEM. ANOVA followed by Tukey's post-hoc analysis was used to compare three or more groups (B), and a two-tailed Student's *t*-test was used to compare two groups (C, D, F, G, I), $^*p < 0.05$, $^{**}p < 0.01$, $^{***}p < 0.001$.

### 2.9. Statistics

Statistical significance was determined by a two-tailed Student's *t*-test or one-way ANOVA. GraphPad Prism 6 was used to analyze the data. Values of $p < 0.05$ were considered statistically significant.

## 3. Results

### 3.1. G-MDSC-derived exosomes attenuate arthritis progression in CIA mice

G-exo and M-MDSC-derived exosomes (M-exo) were derived from spleen G-MDSCs and M-MDSCs of CIA mice, respectively. Neutrophil-derived exosomes (N-exo) were secreted by peripheral blood neutrophils of normal DBA1/J mice. G-exo, M-exo and N-exo were isolated and identified by transmission electron micrography and western blotting (Supplementary Fig. 1). CIA mice were injected with G-exo and M-exo on days 18 and 24 (Fig. 1A). The mean arthritis index (MAI) and the degree of swelling were significantly reduced in the group treated with G-exo, but no obvious changes in these parameters were observed in the group treated with M-exo (Fig. 1B, C). Analysis of the histological scores of joints revealed that G-exo effectively reduced joint damage (Table 1). After treatment with G-exo, the pathological condition of the joints was improved to one of only mild periarticular and fibrovascular synovial proliferation with minimal inflammatory cell infiltration. Moreover, minimal joint damage and intact articular cartilage were observed in the mice treated with G-exo (Fig. 1D). These results showed significantly less severe joint pathology in the mice treated with G-exo than in the mice treated with M-exo or N-exo. Next, we analyzed the percentages of inflammatory Th1 and Th17 cells in the draining lymph nodes. As shown in Fig. 1E, the percentages of Th1 and Th17 cells were significantly lower in the group treated with G-exo than in the groups treated with M-exo or N-exo. However, we did not find a significant change in the proportion of Treg cells in the lymph nodes (data not shown). Consistent with the decreased percentages of Th1 and Th17 cells, the serum levels of IFN-γ and IL-17A were markedly decreased in the group treated with G-exo (Fig. 1E). Generally, the number of lymph node cells was positively correlated with the severity of arthritis. Together, these data suggest that treatment with G-exo attenuates arthritis progression and suppresses the proinflammatory Th1 and Th17 cell response in CIA mice.

### 3.2. G-MDSC-derived exosomes suppress Th1 and Th17 cell differentiation in vitro

Based on the suppression of Th1 and Th17 cells by G-exo in CIA mice, we sought to determine the role of G-exo in the differentiation of Th1 and Th17 cells in vitro. Naïve $CD4^+$ T cells were treated with PKH67-labeled G-exo for 24 h, resulting in an obvious combination of G-exo and naïve $CD4^+$ T cells (Fig. 2A). Under polarized Th1 and Th17 cell differentiation conditions, treatment with G-exo suppressed the differentiation of Th1 and Th17 cells in a dose-dependent manner (Fig. 2B, C, E). Moreover, compared with N-exo, G-exo significantly reduced the levels of IFN-γ and IL-17A (Fig. 2D, F). These results indicated that treatment with G-exo directly suppresses Th1 and Th17 cell differentiation from naïve $CD4^+$ T cells in vitro.

### 3.3. MiR-29a-3p derived from G-MDSC-derived exosomes suppresses Th1 cell differentiation

Exosomes contain abundant lipids, proteins and nucleic acids, and exosomal miRNAs have been reported to play critical biological roles [18]. To determine whether miRNAs in G-exo exerted suppressive effects, we performed miRNA sequence analysis. G-exo contained abundant miRNAs, and the top 20 miRNAs expressed in G-exo are shown (Supplementary Fig. 2A). We then screened 9 candidate miRNAs that could potentially be involved in arthritis and T cell responses. Next, we investigated whether G-exo could directly transfer miRNA to T cells. To this end, G-MDSCs were transfected with a fluorescent Cy-5.5-labeled miRNA mimic, and G-exo containing the Cy-5.5-labeled miRNA mimic (Cy-5.5-G-exo) were isolated. When Cy-5.5-G-exo were added to the culture of naïve $CD4^+$ T cells, the Cy-5.5-labeled miRNA mimic was transferred to $CD4^+$ naïve T cells through transport in G-exo (Supplementary Fig. 2B).

We examined whether miRNAs in G-exo contribute to the induction of Th1 cell responses in vitro. Under polarized Th1 cell differentiation conditions, treatment with G-exo increased miRNA expression in $CD4^+$ T cells. The top 3 candidate miRNAs with the largest fold change after treatment with G-exo were miR-22-3p, miR-16-5p and miR-29a-3p (Fig. 3A). When mimics of the 3 candidate miRNAs were transfected into naïve $CD4^+$ T cells, the percentage of Th1 cells was decreased only in the miR-29a-3p mimic-transfected group under polarized Th1 cell differentiation conditions (Fig. 3B). Moreover, we transfected G-MDSCs with the miR-29a-3p mimic or the miR-29a-3p inhibitor and isolated G-exo. Transfection of the miR-29a-3p mimic significantly increased miR-29a-3p expression in G-MDSCs and G-exo, whereas transfection of the miR-29a-3p inhibitor led to a decrease in the amount of miR-29a-3p packaged in exosomes (Fig. 3C, D). To further examine whether miR-29a-3p derived from G-exo contributes to the suppression of the Th1 cell response, we treated naïve $CD4^+$ T cells with exosomes derived from miR-29a-3p mimic-transfected and miR-29a-3p inhibitor-transfected G-MDSCs under polarized Th1 cell differentiation conditions. G-exo containing the miR-29a-3p mimic significantly suppressed the induction of Th1 cells, whereas G-exo containing the miR-29a-3p inhibitor no longer suppressed the induction of Th1 cells (Fig. 3E, F, G). Recent work reported that miR-29a-3p directly targets T-bet [24]; therefore, we used TargetScan 6.1 software to predict the site on miR-29a-3p that could bind to the 3′-UTR of T-bet (Fig. 3H). Furthermore, western blot analysis indicated that G-exo containing the miR-29a-3p mimic decreased T-bet expression (Fig. 3I). Collectively, these results confirm that miR-29a-3p contributes to the suppression of Th1 cell differentiation mediated by G-exo in vitro.

### 3.4. MiR-93-5p derived from G-MDSC-derived exosomes suppresses Th17 cell differentiation

Likewise, under polarized Th17 cell differentiation conditions, miR-16-5p, miR-29a-3p and miR-93-5p levels were markedly increased after treatment with G-exo (Fig. 4A), and the miR-93-5p mimic reduced the percentage of Th17 cells (Fig. 4B). Treatment with the miR-93-5p mimic significantly increased miR-93-5p expression in both G-MDSCs and G-exo, whereas transfection with the miR-93-5p inhibitor decreased the amount of miR-93-5p packaged in exosomes (Fig. 4C, D).

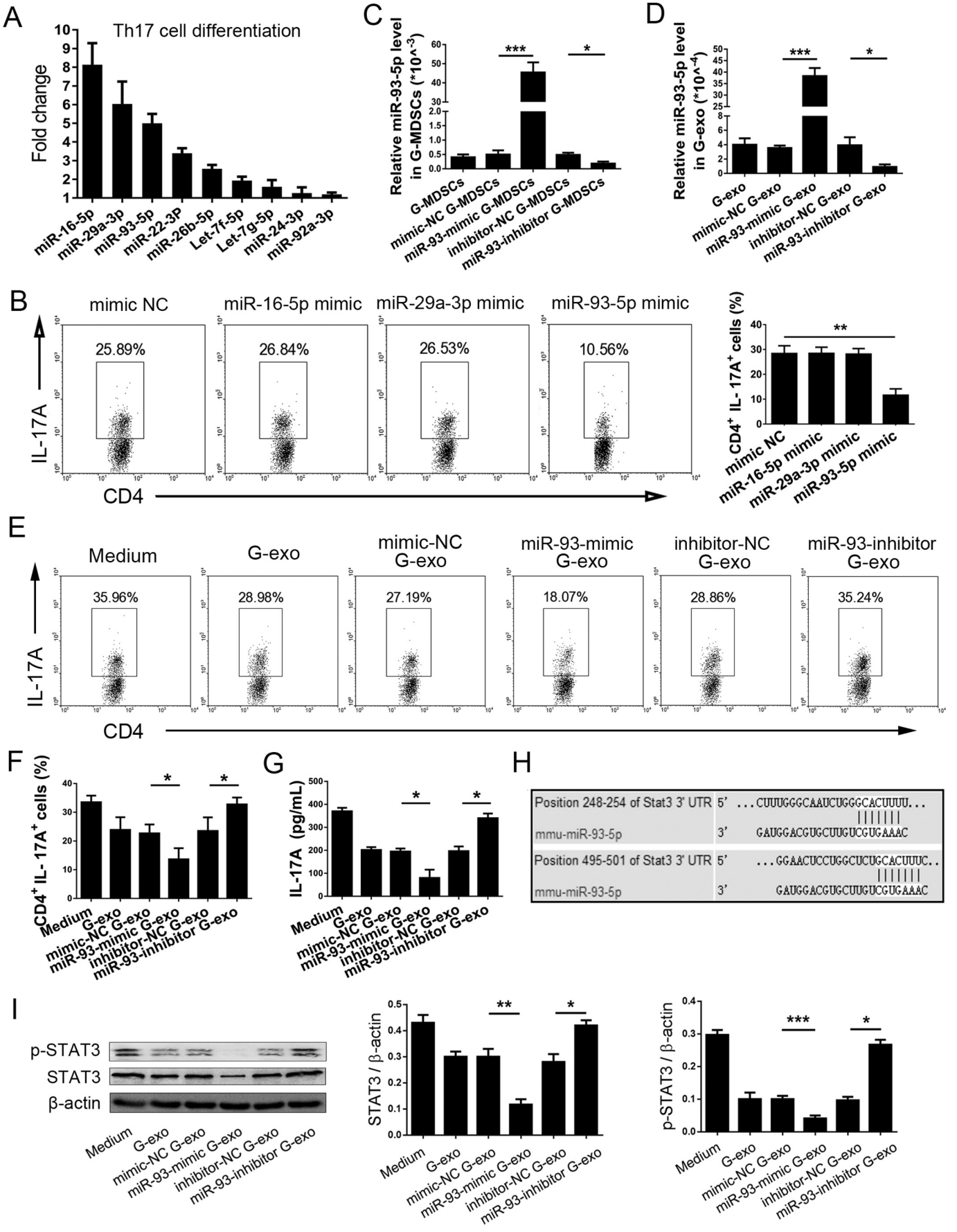


*(caption on next page)*

**Fig. 4.** MiR-93-5p derived from G-MDSC-derived exosomes suppresses Th17 cell differentiation by targeting t-STAT3. (A) The fold changes of the 9 candidate miRNAs after G-exo treatment were determined by qRT-PCR (n = 3). (B) Naïve $CD4^+$ T cells were induced to Th17 cells after transfection with mimic NC, miR-16-5p mimic, miR-29a-3p mimic or miR-93-5p mimic ($n$ = 4). The percentages of Th17 cells were analyzed by FCM (left). The statistical analysis results are shown (right). (C, D) Mimic NC, miR-93-5p mimic, inhibitor NC or miR-93-5p inhibitor was transfected into G-MDSCs, and miR-93-5p levels in G-MDSCs (C) or G-exo (D) were determined by RT-qPCR (n = 4). (E) The frequencies of Th17 cells in the different groups (n = 4) were analyzed by FCM. The statistical analysis of Th17 cell percentages (F) and IL-17A concentrations (G) in the different groups is shown. The results of the statistical analysis of the Th17 cell percentages (F) and IL-17A concentrations (G) in the different groups are shown. (H) The miR-93-5p target sequence in the 3′-UTR of STAT3 was predicted with the TargetScan website. (I) The expression levels of p-STAT3 and STAT3 in the different groups were analyzed by western blotting (left), and the statistical analysis results are shown (right) (n = 3). The values are the means ± SEM. ANOVA followed by Tukey's post-hoc analysis was used to compare three or more groups (B), and a two-tailed Student's $t$-test was used to compare two groups (C, D, F, G, I), $^*p < 0.05$, $^{**}p < 0.01$, $^{***}p < 0.001$.

Exosomes derived from miR-93-5p mimic-transfected G-MDSCs significantly suppressed the induction of Th17 cells. In contrast, exosomes derived from miR-93-5p inhibitor-transfected G-MDSCs no longer suppressed the induction of Th17 cells (Fig. 4E, F, G). According to the results of previous studies and the prediction results from the TargetScan website [25,26], miR-93-5p can bind to the 3′-UTR of STAT3 (Fig. 4H). Western blot analysis showed that miR-93-5p derived from G-exo decreased the expression of STAT3 (Fig. 4I). These results suggest that miR-93-5p derived from G-exo suppresses Th17 differentiation by targeting STAT3.

### 3.5. Exogenous miR-29a-3p and miR-93-5p derived from bone marrow G-MDSC-derived exosomes attenuate arthritis progression in CIA mice

The above in vitro and in vivo experiments clarified that treatment with G-exo suppresses Th1 and Th17 cell responses in CIA. Due to our findings with G-exo derived from CIA mice, we attempted to isolate G-exo from healthy mice. To this end, we induced G-MDSCs from bone marrow cells (BM-G-MDSCs) with GM-CSF and IL-6, and we then successfully isolated G-MDSCs with microbeads at a purity of > 90% (Fig. 5A). Subsequently, we cotransfected BM-G-MDSCs with the miR-29a-3p mimic and miR-93-5p mimic and isolated exosomes containing the miR-29/93 mimics (Fig. 5B, C). CIA mice were injected intravenously with BM-G-MDSC-derived exosomes (BM-G-exo) on days 18 and 24. BM-G-exo delayed the progression of CIA and reduced the degree of swelling (Fig. 5D, E). Moreover, synovial hyperplasia, leukocyte infiltration and bone destruction were significantly milder in the group treated with BM-G-exo than in the control group (Fig. 5F, Table 2). As shown in Fig. 5G, the percentages of Th1 and Th17 cells in the group treated with BM-G-exo were lower than those in the control group. Furthermore, the serum levels of IFN-γ and IL-17A were decreased in the group treated with BM-G-exo. Excitingly, the miR-29/93-mimic BM-G-exo had a stronger ability to protect joints than BM-G-exo according to the above indicators (Fig. 5D, F, Table 2). In addition, BM-G-exo decreased the levels of T-bet and STAT3 in $CD4^+$ T cells from the draining lymph nodes, and the miR-29/93-mimic BM-G-exo inhibited the expression of T-bet and STAT3 more effectively in CIA mice (Supplementary Fig. 3). Together, these data demonstrated that the exogenous miR-29/93-mimics derived from BM-G-exo exert immunosuppressive effects that ameliorate autoimmune progression in CIA mice.

### 3.6. Human MDSC-derived exosomes suppress Th1 and Th17 cell differentiation in vitro through miR-29a-3p and miR-93-5p

Since murine G-exo suppresses Th1 and Th17 cell responses, we further examined the suppression of Hu-MDSC-exo on Th1 and Th17 cell differentiation in vitro. Human peripheral blood mononuclear cells (PBMCs) were cultured with GM-CSF and IL-1β, and human MDSCs (Hu-MDSCs) were isolated and identified to have the $CD33^+CD11b^+HLA\text{-}DR^{low}$ phenotype [27,28] (Fig. 6A). According to TargetScan analysis and the results of related studies (Supplementary Fig. 3A, B), miR-29a-3p and miR-93-5p target T-bet and STAT3, respectively, in both humans and mice [29,30]. Mimics and inhibitors of miR-29a-3p and miR-93-5p were transfected into Hu-MDSCs (Fig. 6B, D), and exosomes secreted by Hu-MDSCs were isolated and identified (Fig. 6C, E). Naïve $CD4^+$ T cells were treated with Hu-MDSC-derived exosomes (Hu-MDSC-exo) under polarized Th1 and Th17 cell differentiation conditions, as described in the methods section. Exosomes derived from miR-29a-3p mimic-transfected Hu-MDSCs significantly suppressed the induction of Th1 cells. In contrast, exosomes derived from miR-29a-3p inhibitor-transfected Hu-MDSCs no longer suppressed the induction of Th1 cells (Fig. 6F, G). Hu-MDSC-exo containing the miR-93-5p mimic significantly suppressed the induction of Th17 cells, whereas Hu-MDSC-exo containing the miR-93-5p inhibitor no longer suppressed the induction of Th17 cells (Fig. 6F, H). Taken together, these data indicate that Hu-MDSC-exo suppress Th1 and Th17 cell differentiation through exosomal miR-29a-3p and miR-93-5p.

## 4. Discussion

Although studies on MDSCs have traditionally focused on cancer patients and tumor models, researchers initially found that MDSCs accumulate in autoimmune disease and play an important role in inflammation [31]. Fujii and colleagues showed that MDSCs could accumulate in the spleen of CIA mice and suppress inflammation via the inhibition of $CD4^+$ T cells, and they also tried to alleviate CIA in mice via the adoptive transfer of MDSCs [32]. However, another study showed that MDSCs promote the differentiation of Th17 cells via IL-1β and aggravate inflammation in CIA mice [33]. These contradictory conclusions might stem from differences in pathogenesis, MDSC subpopulations, microenvironments and mouse genetic backgrounds among the studies. Overall, the exact role of MDSCs in the pathogenesis of CIA in mice remains to be validated, and the therapeutic effect of adoptive MDSC transfer is still controversial.

Accumulating evidence has shown that exosomes play important roles in intercellular signaling [34]. Compared to the use of parental cells, the use of exosomes to regulate recipient cells has many advantages [35,36]. First, exosomes can be easily stored and transported. Second, exosomes have minimal cytotoxicity and antigenicity. Finally, exosomal cargos can be stably transported to specific tissues and organs via body fluids. In addition, current experimental results show that there are differences in the functions of MDSCs in different stages of CIA mice [32,33]. Compared with MDSCs, the components and functions of exosomes derived from MDSCs should be more stable. We isolated exosomes derived from MDSCs, namely, G-MDSCs and M-MDSCs. We found that G-exo and M-exo are small vesicles 30–150 nm in diameter with high expression of CD9 and CD63. These characteristics, which correspond with the characteristics of exosomes shown in a previous study, suggested that G-exo and M-exo were successfully isolated [34]. Considering the advantages of exosome treatment for disease, we administered MDSC-derived exosomes to CIA mice and found that only G-exo effectively attenuated CIA and reduced the proportions of Th1 and Th17 cells in the draining lymph nodes; M-exo lost this suppressive ability. Moreover, our results demonstrated that G-exo inhibit Th1 and Th17 cell differentiation in vitro. Thus, our work provides evidence that administration of G-MDSC-derived exosomes exerts an immunosuppressive effect in mice with inflammatory arthritis. However, exosomes secreted by G-MDSCs from CIA mice themselves are apparently not sufficient to prevent arthritis progression in vivo. We

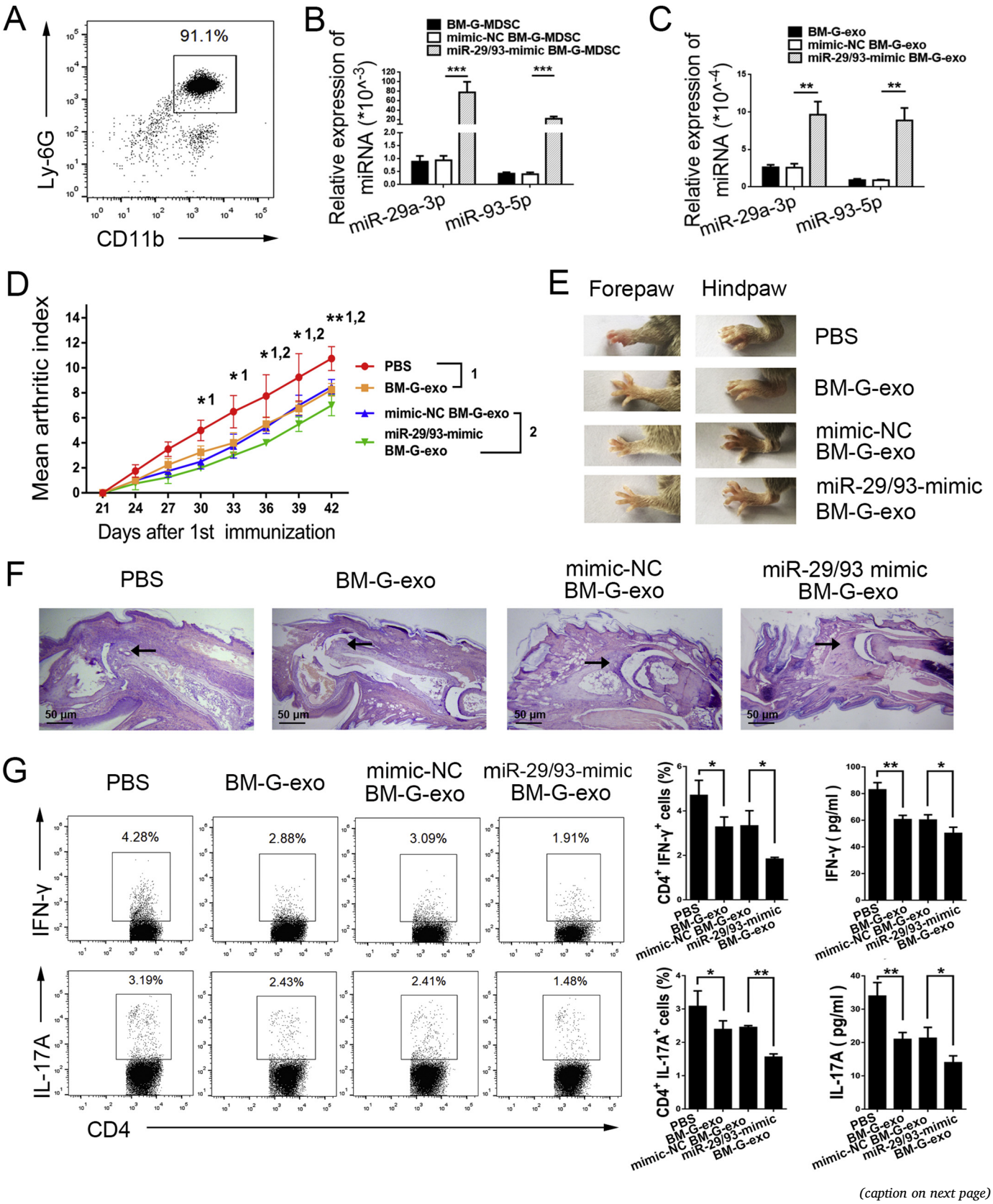


*(caption on next page)*

speculated that exosomes secreted by G-MDSCs from CIA mice did not reach the dose threshold for inhibiting inflammation. In addition, there are differences in the functions of MDSCs in mice at different stages of CIA, and the components of G-exo produced in CIA mice may vary at different stages of disease.

A report showed that MDSC-derived exosomes packaged different proteins, mRNAs, and miRNAs from MDSCs, indicating a potential complex immunomodulatory function [37]. Various studies have

**Fig. 5.** Exosomes derived from G-MDSCs induced by bone marrow cells attenuate collagen-induced arthritis. (A) Mouse bone marrow cells were induced to $CD11b^+Ly\text{-}6G^+$ G-MDSCs by culturing for 6 days in the presence of 20 ng/ml GM-CSF and 10 ng/ml IL-6. $CD11b^+Ly\text{-}6G^+$ BM-G-MDSCs were sorted by FCM. (B, C) BM-G-MDSCs were transfected with the miR-29a-3p mimic and miR-93-5p mimic, and the miR-29a-3p and miR-93-5p levels in the BM-G-MDSCs (B) or BM-G-exo (C) were determined by RT-qPCR (n = 4). CIA mice were administered BM-G-exo (100 μg/mouse/injection) on days 18 and 24 ($n$ = 6). The mice were sacrificed on day 42 for subsequent experiments. (D) The development of arthritis in CIA mice treated with BM-G-exo was monitored every 3 days. (E) Representative images of the forepaws and hindpaws from the different groups are shown. (F) Representative hematoxylin-eosin-stained sections of joint tissues are shown (original magnification, ×100). (G) The percentages of Th1 and Th17 cells in the draining lymph nodes were analyzed by FCM (n = 6). The concentrations of serum IFN-γ and IL-17A in the different groups were measured by ELISA (n = 6). The values are the means ± SEM. Two-tailed Student's $t$-test was used to compare two groups (B, C), and ANOVA followed by Tukey's post-hoc analysis was used to compare three or more groups (D, G), $^*p < 0.05$, $^{**}p < 0.01$, $^{***}p < 0.001$.

**Table 2**
Histological scores of ankle joints in BM-G-exosome-treated CIA mice.

| | Synovial hyperplasia | Cell infiltration | Pannus | Inflammation | Bone erosion |
|---|---|---|---|---|---|
| PBS | 2.50 ± 0.45 | 2.00 ± 0.31 | 2.16 ± 0.72 | 1.67 ± 0.35 | 2.67 ± 0.65 |
| BM-G-exo | 1.33 ± 0.12** | 1.17 ± 0.21** | 1.00 ± 0.33** | 1.17 ± 0.27* | 1.33 ± 0.68*,A |
| Mimic-NC-exo | 1.50 ± 0.26 | 1.33 ± 0.44 | 1.17 ± 0.31 | 1.17 ± 0.21 | 1.50 ± 0.20 |
| MiR-29/93-exo | 0.83 ± 0.21* | 0.83 ± 0.16* | 0.67 ± 0.26* | 0.50 ± 0.12** | 0.83 ± 0.11*,B |

The value is the mean ± SEM (n = 6). ANOVA followed by Tukey's post-hoc analysis was used to compare three or more groups, *p < 0.05, **P < 0.01 (A: BM-G-exo versus PBS; B: MiR-29/93-exo versus Mimic-NC-exo). Note: BM-G-exo, exosomes derived from granulocytic myeloid-derived suppressor cells induced from bone marrow cells; Mimic-NC-exo, exosomes derived from mimic negative control-transfected granulocytic myeloid-derived suppressor cells induced from bone marrow cells; MiR-29/93-exo, exosomes derived from miR-29a-3p and miR-93-5p mimic-transfected granulocytic myeloid-derived suppressor cells induced from bone marrow cells.

shown that miRNAs regulate the differentiation and function of helper T cells by inhibiting the transcription of mRNA [38]. Exosomes can transfer miRNAs to target cells and regulate gene expression to affect the function of these recipient cells [39]. We cannot rule out the possibility that G-exo contain some other molecules that protect CIA mice, but miRNAs were selected as the focus of our study according to the current literature. Next, we performed miRNA sequence analysis on G-exo and screened out miR-16-5p, miR-29a-3p, miR-93-5p, miR-22-3p, and Let-7 g-5p from the top twenty miRNAs with the largest fold change after treatment with G-exo as contributors to osteoarthritis development and osteoblast proliferation, differentiation and migration [40–43]. MiR-22-3p and miR-26b-5p were reported to be involved in the pathogenesis of RA [44–46]. Moreover, miR-29a-3p, miR-93-5p and miR-24-3p were found to be related to the proliferation, differentiation and immune response of T cells [20,24,25]. TargetScan software was then used to predict the targets of the top 20 miRNAs. MiR-16-5p, miR-29a-3p, Let-7f-5p, and miR-92a-3p were found to target Smad7, Smad6, FOS, T-bet, PIK3R1, t-STAT3 and EMOS, which are related to the proliferation and differentiation of T cells [47–50]. Finally, miR-16-5p, miR-29a-3p, miR-93-5p, miR-22-3p, miR-26b-5p, Let-7f-5p, Let-7 g-5p, miR-24-3p, and miR-92a-3p were selected as candidate miRNAs.

Further experiments showed that the proportion of Th1 cells was decreased in the group treated with miR-29-mimic-containing G-exo, while the proportion of Th1 cells was increased in the group treated with miR-29-inhibitor-containing G-exo. According to TargetScan, T-bet is the direct target of miR-29a-3p, as identified in a previous study [24]. Western blotting indicated that the miR-29a-3p derived from G-exo reduced the level of T-bet. Thus, these results demonstrate that miR-29a-3p derived from G-exo suppressed Th1 differentiation by targeting T-bet. Via the same process, miR-93-5p derived from G-exo was shown to suppress Th17 cell differentiation. In fact, STAT3 plays an important role in Th17 cell differentiation in at least four ways, and STAT3 can directly bind and regulate IL-17a, IL-17f and IL-21, as well as regulate the expression of ROR-γt and IL-23R [51–55]. According to TargetScan 6.1 software, STAT3 is the direct target of miR-93-5p, as demonstrated by other researchers [25,56]. Furthermore, miR-93-5p derived from G-exo was found to suppress Th17 cell differentiation by targeting STAT3. Although miR-29a-3p and miR-93-5p derived from G-exo were shown to inhibit Th1 and Th17 cell differentiation, we did not exclude the possibility of other specific mechanisms by which G-exo play a role in protection against arthritis. In addition, it is entirely possible because exosomes contain a variety of biological components. Compared with the exosomes derived from neutrophils and M-MDSCs, G-MDSCs-exo can play a protective role in arthritis, which is a problem worthy of further study.

The use of exosomes carrying drugs, miRNAs and proteins as therapeutic agents has been attempted [57]. In one study, HEK293T cell-secreted exosomes were engineered to express high levels of miR-199a via a special TAT peptide-TAR interaction [58]. In our study, miR-29a-3p and miR-93-5p derived from G-exo alleviated CIA by inhibiting Th1 and Th17 cell responses. However, the source of G-MDSCs has always been a concern. Exosomes derived from bone marrow culture-induced G-MDSCs will be safer and more convenient in therapeutic application than will exosomes derived by other means. Interestingly, exogenous miR-29a-3p and miR-93-5p derived from BM-G-exo may play a similar role in attenuating CIA. According to the prediction results from TargetScan and the findings from current papers, T-bet and STAT3 are the direct targets of miR-29a-3p and miR-93-5p in humans, respectively [29,30]. As expected, Hu-MDSC-exo suppressed Th1 and Th17 cell differentiation, which suggests that MDSC-derived exosomes have therapeutic potential in RA and other autoimmune diseases. Thus, this study reveals a novel non-cell-based therapeutic strategy in autoimmune disease.

## Transparency document

The Transparency document associated with this article can be found, in online version.

## Funding

This work was supported by the National Natural Science Foundation of China (Grant Nos. 31470881, 31711530025, and 81771759), Jiangsu Province's Key Medical Talents Program (Grant No. ZDRCB2016018), and the Jiangsu Province “333” Project (Grant No. BRA2017128), and Project Funded by the Priority Academic Program Development of Jiangsu Higher Education Institutions.

## Author contributions

SW and JT designed the experiments; DZ, JT, XW and ML performed the experiments; and DZ, XT, KR, HG, and JM analyzed the data. SW and XH supervised the research. DZ and SW wrote the manuscript.

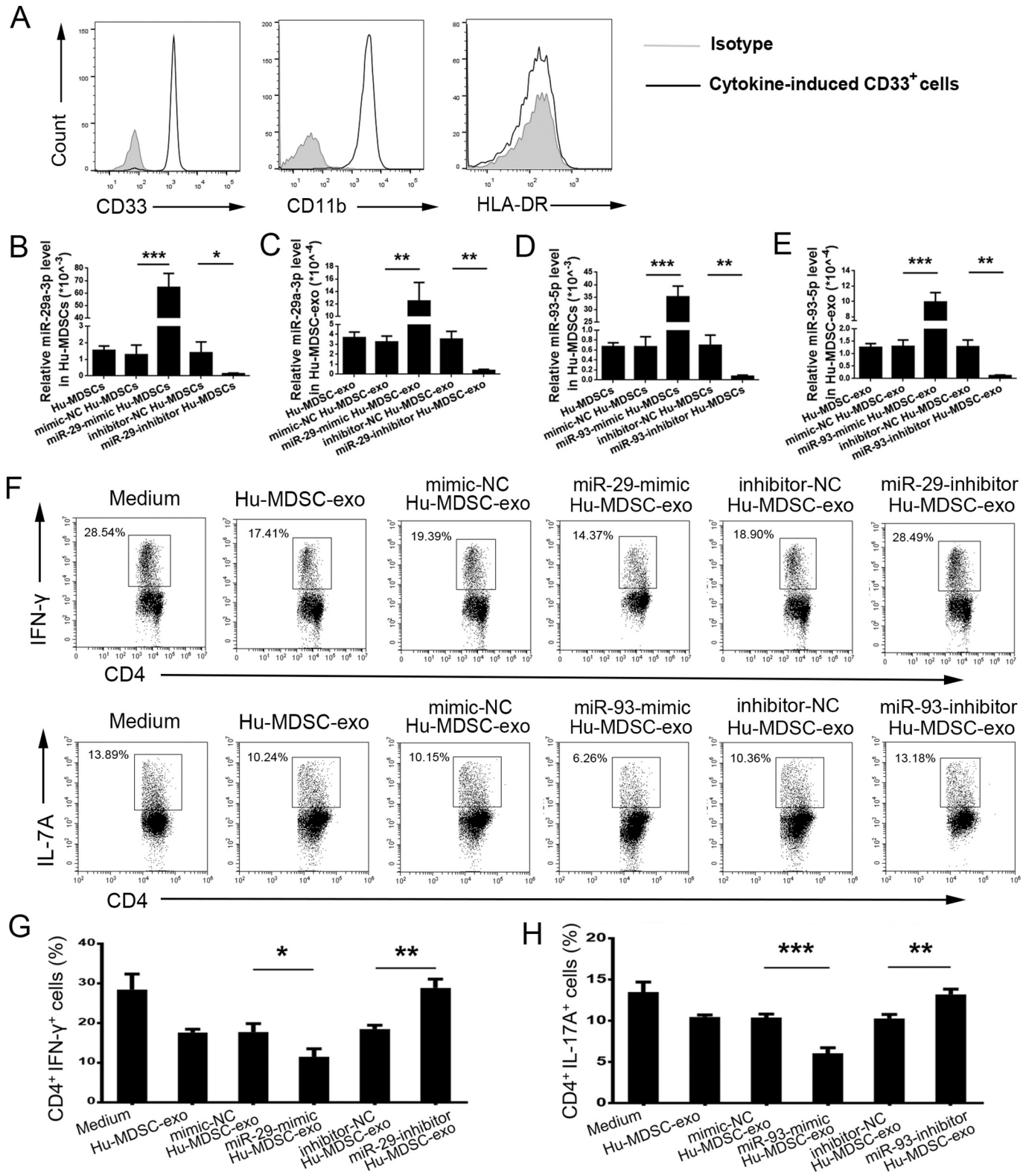


**Fig. 6.** Human MDSC-derived exosomes suppress Th1 and Th17 cell differentiation in vitro. (A) Hu-MDSCs were induced from healthy human PBMCs by culturing for 6 days in the presence of 40 ng/ml GM-CSF and 10 ng/ml IL-1β, and CD33, CD11b and HLA-DR phenotypes were analyzed by FCM. Mimic NC, miR-29a-3p mimic, inhibitor NC or miR-29a-3p inhibitor was transfected into Hu-MDSCs, and miR-29a-3p levels in Hu-MDSCs (B) or Hu-MDSC-exo (C) were determined by RT-qPCR (n = 4). Mimic NC, miR-93-5p mimic, inhibitor NC or miR-93-5p inhibitor was transfected into Hu-MDSCs, and miR-93-5p levels in Hu-MDSCs (D) or Hu-MDSC-exo (E) were determined by RT-qPCR (n = 4). (F) The frequencies of Th1 and Th17 cells in the different groups (n = 4) were analyzed by FCM. The statistical analysis results of Th1 cells (G) and Th17 cells (H) are shown. The values are the means ± SEM. Two-tailed Student's *t*-test was used to compare two groups (B, C, D, E), and ANOVA followed by Tukey's post-hoc analysis was used to compare three or more groups (G, H), $^{*}p < 0.05$, $^{**}p < 0.01$, $^{***}p < 0.001$.

## Declaration of competing interest

The authors have declared that no conflicts of interest exist.

## Acknowledgments

We thank Dr. M. Chen for histopathological examination and D. Feng and J. Mao for flow cytometric testing.

## Appendix A. Supplementary data

Supplementary data to this article can be found online at https://doi.org/10.1016/j.bbadis.2019.165540.

## References

[1] J.S. Smolen, D. Aletaha, A. Barton, et al., Rheumatoid arthritis, Nat. Rev. Dis. Primers. 4 (2018) 18001.
[2] G.S. Firestein, I.B. Mcinnes, Immunopathogenesis of rheumatoid arthritis, Immunity 46 (2) (2017) 183–196.
[3] I.B. Mcinnes, G. Schett, The pathogenesis of rheumatoid arthritis, N. Engl. J. Med. 365 (23) (2011) 2205–2219.
[4] S. Wang, Y. Shi, M. Yang, et al., Glucocorticoid-induced tumor necrosis factor receptor family-related protein exacerbates collagen-induced arthritis by enhancing the expansion of Th17 cells, Am. J. Pathol. 180 (3) (2012) 1059–1067.
[5] A.P. Cope, Emerging therapies for pre-RA, Best Pract. Res. Clin. Rheumatol. 31 (1) (2017) 99–111.
[6] J.S. Smolen, R. Landewe, J. Bijlsma, et al., EULAR recommendations for the management of rheumatoid arthritis with synthetic and biological disease-modifying antirheumatic drugs: 2016 update, Ann. Rheum. Dis. 76 (6) (2017) 960–977.
[7] D.I. Gabrilovich, S. Nagaraj, Myeloid-derived suppressor cells as regulators of the immune system, Nat. Rev. Immunol. 9 (3) (2009) 162–174.
[8] X. Tian, J. Ma, T. Wang, et al., Long non-coding RNA HOXA transcript antisense RNA myeloid-specific 1-HOXA1 axis downregulates the immunosuppressive activity of myeloid-derived suppressor cells in lung cancer, Front. Immunol. 9 (2018) 473.
[9] J.I. Youn, S. Nagaraj, M. Collazo, D.I. Gabrilovich, Subsets of myeloid-derived suppressor cells in tumor-bearing mice, J. Immunol. 181 (8) (2008) 5791–5802.
[10] W. Fujii, E. Ashihara, H. Hirai, et al., Myeloid-derived suppressor cells play crucial roles in the regulation of mouse collagen-induced arthritis, J. Immunol. 191 (3) (2013) 1073–1081.
[11] H. Zhang, Y. Huang, S. Wang, et al., Myeloid-derived suppressor cells contribute to bone erosion in collagen-induced arthritis by differentiating to osteoclasts, J. Autoimmun. 65 (2015) 82–89.
[12] J. Tian, et al., Increased GITRL impairs the function of myeloid-derived suppressor cells and exacerbates primary Sjögren's syndrome, J. Immunol. 202 (6) (2019) 1693–1703.
[13] K.R. Crook, M. Jin, M.F. Weeks, et al., Myeloid-derived suppressor cells regulate T cell and B cell responses during autoimmune disease, J. Leukoc. Biol. 97 (3) (2015) 573–582.
[14] Y. Wang, J. Tian, S. Wang, The potential therapeutic role of myeloid-derived suppressor cells in autoimmune arthritis, Semin. Arthritis Rheum. 45 (4) (2016) 490–495.
[15] Y. Wang, K. Yin, J. Tian, et al., Granulocytic myeloid-derived suppressor cells promote the stemness of colorectal cancer cells through exosomal S100A9, Adv. Sci. 2019 (6) (2019) 1901278.
[16] M. Record, C. Subra, S. Silvente-Poirot, M. Poirot, Exosomes as intercellular signalosomes and pharmacological effectors, Biochem. Pharmacol. 81 (10) (2011) 1171–1182.
[17] Y. Wang, J. Tian, X. Tang, et al., Exosomes released by granulocytic myeloid-derived suppressor cells attenuate DSS-induced colitis in mice, Oncotarget 7 (13) (2016) 15356–15368.
[18] J. Zhang, S. Li, L. Li, et al., Exosome and exosomal microRNA: trafficking, sorting, and function, Genomics Proteomics Bioinformatics 13 (1) (2015) 17–24.
[19] I.S. Okoye, S.M. Coomes, V.S. Pelly, et al., MicroRNA-containing T-regulatory-cell-derived exosomes suppress pathogenic T helper 1 cells, Immunity 41 (1) (2014) 89–103.
[20] S.B. Ye, H. Zhang, T.T. Cai, et al., Exosomal miR-24-3p impedes T-cell function by targeting FGF11 and serves as a potential prognostic biomarker for nasopharyngeal carcinoma, J. Pathol. 240 (3) (2016) 329–340.
[21] N.A. Sims, J.R. Green, M. Glatt, et al., Targeting osteoclasts with zoledronic acid prevents bone destruction in collagen-induced arthritis, Arthritis Rheum. 50 (7) (2004) 2338–2346.
[22] L.A. Joosten, S. Abdollahi-Roodsaz, M. Heuvelmans-Jacobs, et al., T cell dependence of chronic destructive murine arthritis induced by repeated local activation of toll-like receptor-driven pathways: crucial role of both interleukin-1beta and interleukin-17, Arthritis Rheum. 58 (1) (2008) 98–108.
[23] Y. Zheng, X. Tian, T. Wang, et al., Long noncoding RNA Pvt1 regulates the immunosuppression activity of granulocytic myeloid-derived suppressor cells in tumor-bearing mice, Mol. Cancer 18 (2019) 61.
[24] D.F. Steiner, M.F. Thomas, J.K. Hu, et al., MicroRNA-29 regulates T-box transcription factors and interferon-gamma production in helper T cells, Immunity 35 (2) (2011) 169–181.
[25] K.M. Foshay, G.I. Gallicano, miR-17 family miRNAs are expressed during early mammalian development and regulate stem cell differentiation, Dev. Biol. 326 (2) (2009) 431–443.
[26] X.T. Yan, L.J. Ji, Z. Wang, et al., MicroRNA-93 alleviates neuropathic pain through targeting signal transducer and activator of transcription 3, Int. Immunopharmacol. 46 (2017) 156–162.
[27] P. Serafini, I. Borrello, V. Bronte, Myeloid suppressor cells in cancer: recruitment, phenotype, properties, and mechanisms of immune suppression, Semin. Cancer Biol. 16 (1) (2006) 53–65.
[28] S. Ugel, F. Delpozzo, G. Desantis, et al., Therapeutic targeting of myeloid-derived suppressor cells, Curr. Opin. Pharmacol. 9 (4) (2009) 470–481.
[29] S. Liu, S.H. Patel, C. Ginestier, et al., MicroRNA93 regulates proliferation and differentiation of norm-al and malignant breast stem cells, PLoS Genet. 8 (6) (2012) e1002751.
[30] Y. Xiang, X.H. Liao, C.X. Yu, et al., MiR-93-5p inhibits the EMT of breast cancer cells via targeting MK-L-1 and STAT3, Exp. Cell Res. 357 (1) (2017) 135–144.
[31] L.B. Nicholson, B.J. Raveney, M. Munder, Monocyte dependent regulation of autoimmune inflammation, Curr. Mol. Med. 9 (1) (2009) 23–29.
[32] L. Zhang, Z. Zhang, H. Zhang, M. Wu, Y. Wang, Myeloid-derived suppressor cells protect mouse models from autoimmune arthritis via controlling inflammatory response, Inflammation 37 (3) (2014) 670–677.
[33] H. Zhang, S. Wang, Y. Huang, et al., Myeloid-derived suppressor cells are proinflammatory and regulate collagen-induced arthritis through manipulating Th17 cell differentiation, Clin. Immunol. 157 (2) (2015) 175–186.
[34] K. Boriachek, M.N. Islam, A. Moller, et al., Biological functions and current advances in isolation and detection strategies for exosome nanovesicles, Small (2018) 14(6).
[35] V. Borger, M. Bremer, R. Ferrer-Tur, et al., Mesenchymal stem/stromal cell-derived extracellular vesicles and their potential as novel immunomodulatory therapeutic agents, Int. J. Mol. Sci. (2017) 18(7).
[36] A. Jarmalaviciute, A. Pivoriunas, Exosomes as a potential novel therapeutic tools against neurodeg-enerative diseases, Pharmacol. Res. 113 (Pt B) (2016) 816–822.
[37] L. Geis-Asteggiante, A.T. Belew, V.K. Clements, et al., Differential content of proteins, mRNAs, and miRNAs suggests that MDSC and their exosomes may mediate distinct immune suppressive functions, J. Proteome Res. 17 (1) (2018) 486–498.
[38] A. Mehta, D. Baltimore, MicroRNAs as regulatory elements in immune system logic, Nat. Rev. Immunol. 16 (5) (2016) 279–294.
[39] H. Valadi, K. Ekstrom, A. Bossios, M. Sjostrand, J.J. Lee, J.O. Lotvall, Exosome-mediated transfer of mRNAs and microRNAs is a novel mechanism of genetic exchange between cells, Nat. Cell Biol. 9 (6) (2007) 654–659.
[40] L. Li, J. Jia, X. Liu, et al., MicroRNA-16-5p controls development of osteoarthritis by targeting SMAD-3 in chondrocytes, Curr. Pharm. Des. 21 (35) (2015) 5160–5167.
[41] L.T. Le, T.E. Swingler, N. Crowe, et al., The microRNA-29 family in cartilage homeostasis and osteoarthritis, J. Mol. Med. (Berl) 94 (5) (2016) 583–596.
[42] W.H. Yang, C.H. Tsai, Y.C. Fong, et al., Leptin induces oncostatin M production in osteoblasts by downregulating miR-93 through the Akt signaling pathway, Int. J. Mol. Sci. 15 (9) (2014) 15778–15790.
[43] S. Weilner, S. Skalicky, B. Salzer, et al., Differentially circulating miRNAs after recent osteoporotic fractures can influence osteogenic differentiation, Bone 79 (2015) 43–51.
[44] L. Ouboussad, L. Hunt, E.M.A. Hensor, et al., Profiling microRNAs in individuals at risk of progression to rheumatoid arthritis, Arthritis Res. Ther. 19 (1) (2017) 288.
[45] P. Fan, L. He, N. Hu, et al., Effect of 1,25-(OH)2D3 on proliferation of fibroblast-like synoviocytes and expressions of pro-inflammatory cytokines through regulating MicroRNA-22 in a rat model of rheumatoid arthritis, Cell. Physiol. Biochem. 42 (1) (2017) 145–155.
[46] T. Niimoto, T. Nakasa, M. Ishikawa, et al., MicroRNA-146a expresses in interleukin-17 producing T cells in rheumatoid arthritis patients, BMC Musculoskelet. Disord. 11 (2010) 209.
[47] M.A. Honardoost, R. Naghavian, F. Ahmadinejad, A. Hosseini, K. Ghaedi, Integrative computational mRNA-miRNA interaction analyses of the autoimmune-deregulated miRNAs and well-known Th1-7 differentiation regulators: an attempt to discover new potential miRNAs involved in Th17 differentiation, Gene 572 (2) (2015) 153–162.
[48] C. Gutierrez-Vazquez, A. Rodriguez-Galan, M. Fernandez-Alfara, et al., miRNA profiling during antigen-dependent T cell activation: a role for miR-132-3p, Sci. Rep. 7 (1) (2017) 3508.
[49] M.C. Deau, L. Heurtier, P. Frange, et al., A human immunodeficiency caused by mutations in the PIK-3R1 gene, J. Clin. Invest. 124 (9) (2014) 3923–3928.
[50] K. Chemin, D. Ramskold, L.M. Diaz-Gallo, et al., EOMES-positive CD4+ T cells are increased in PTPN22 (1858T) risk allele carriers, Eur. J. Immunol. 48 (4) (2018) 655–699.
[51] L. Zhou, Ii Ivanov, R. Spolski, et al., IL-6 programs T(H)-17 cell differentiation by promoting sequential engagement of the IL-21 and IL-23 pathways, Nat. Immunol. 8 (9) (2007) 967–974.
[52] Z. Chen, C.M. Tato, L. Muul, et al., Distinct regulation of interleukin-17 in human T helper lymphocytes, Arthritis Rheum. 56 (9) (2007) 2936–2946.
[53] A.N. Mathur, H.C. Chang, D.G. Zisoulis, et al., Stat3 and Stat4 direct development of IL-17-secreting Th cells, J. Immunol. 178 (8) (2007) 4901–4907.
[54] Z. Chen, A. Laurence, Y. Kanno, et al., Selective regulatory function of Socs3 in the formation of IL-17-secreting T cells, Proc. Natl. Acad. Sci. U. S. A. 103 (21) (2006) 8137–8142.
[55] L. Wei, A. Laurence, K.M. Elias, et al., IL-21 is produced by Th17 cells and drives IL-17 production in a STAT3-dependent manner, J. Biol. Chem. 282 (48) (2007)

34605–34610.
[56] Q. Cui, H. Shi, P. Ye, et al., m(6)A RNA methylation regulates the self-renewal and tumorigenesis of glioblastoma stem cells, Cell Rep. 18 (11) (2017) 2622–2634.
[57] A.A. Farooqi, N.N. Desai, M.Z. Qureshi, et al., Exosome biogenesis, bioactivities and functions as new delivery systems of natural compounds, Biotechnol. Adv. 36 (1) (2018) 328–334.
[58] D.S. Sutaria, J. Jiang, O.A. Elgamal, et al., Low active loading of cargo into engineered extracellular vesicles results in inefficient miRNA mimic delivery, J. Extracell. Vesicles 6 (1) (2017) 1333882.